Reprinted from Journal of Biomechanics, Vol 35, Calonius, O. and Saikko, V.,
Slide track analysis of eight contemporary hip simulator designs,
Pages 1439-1450 Copyright (2002), with permission from Elsevier Science.

ELSEVIER

Journal of Biomechanics 35 (2002) 1439–1450

JOURNAL OF BIOMECHANICS

www.elsevier.com/locate/jbiomech
www.JBiomech.com

Slide track analysis of eight contemporary hip simulator designs

Olof Calonius, Vesa Saikko*

Department of Mechanical Engineering, Helsinki University of Technology, Laboratory of Machine Design, P.O. Box 4300, FIN-02015 HUT, Finland

Accepted 21 June 2002

Abstract

In an earlier paper, the authors presented a new method of computation of slide tracks in the relative motion between femoral head and acetabular cup of total hip prostheses. For the first time, computed tracks were verified experimentally and with an alternative method of computation. Besides being an efficient way to illustrate hip kinematics, the shapes of the slide tracks are known to be of fundamental importance regarding the wear behaviour of prostheses. The verified method was now applied to eight contemporary hip simulator designs. The use of correct motion waveforms and an Euler sequence of rotations in each case was again found to be essential. Considerable differences were found between the simulators. For instance, the shapes of the tracks drawn by the resultant contact force included a circle, ellipse, irregular oval, leaf, twig, and straight line. Computation of tracks correctly for the most widely used hip simulator, known as biaxial, was made possible by the insight that the device is actually three-axial. Slide track patterns have now been computed for virtually all contemporary hip simulators, and both for the heads and for the cups. This comparative analysis forms a valuable basis for studies on the relationship between the type of multidirectional motion and wear. These studies can produce useful information for the design of joint simulators, and improve the understanding of wear phenomena in prosthetic joints.

Keywords: Slide track; Hip simulator; Euler angle; Multidirectional motion; Wear

1. Introduction

In an earlier study (Saikko and Calonius, 2002), a new method of computation of slide tracks in the relative motion between femoral head and acetabular cup was presented. Slide tracks are an efficient way to illustrate hip kinematics in various activities, and in different hip simulators used in wear testing of total hip prostheses. The shape of the track specifies how the direction of sliding changes during the activity, e.g., a walking cycle. The change with time of the direction of sliding is known to be of fundamental importance regarding the wear of the prosthesis (Bennett et al., 2000; Saikko and Ahlroos, 1999). For the first time, tracks were computed for both the head and the cup, and were verified experimentally, and by using an alternative method of computation. The simulators analysed were the three-axis HUT-3 and biaxial rocking motion (BRM) with a zero-offset rotation-prevention lever. The verification was done by embedding several sharp pins into acetabular cups, which were then installed in the simulators. The pins carved grooves on the heads as one complete cycle was driven with the load on. The carved grooves were found to be identical with the computed tracks. The two methods of computation were found to produce identical tracks.

The computed simulator tracks were compared with those computed from a goniometric study of three-axis hip joint motion in level walking (Johnston and Smidt, 1969). The tracks produced by the HUT-3 simulator were found to agree well with the gait tracks. The increase of the aspect ratio of the tracks on the high contact pressure zone was shown to decrease the wear rate of polyethylene acetabular cup against polished CoCr head in serum lubrication. The gait tracks differed from those computed by Ramamurti et al. (1996). Moreover, the tracks computed for the BRM simulator clearly differed from those computed by Ramamurti et al. (1998). The use of a correct Euler sequence of rotations was found to be essential. Ramamurti et al.

*Corresponding author. Tel.: +358-9-451-3562; fax: +358-9-451-3542.

E-mail address: vesa.saikko@hut.fi (V. Saikko).

0021-9290/02/$ - see front matter
PII: S0021-9290(02)00171-9

Nomenclature

L	joint contact resultant force
r	radius of femoral head
t	time
T	cycle time
τ_μ	tangential shear stress at articulating surface caused by friction
FE	flexion-extension
AA	abduction–adduction
IER	internal–external rotation
BRM	biaxial rocking motion
HUT-3	Helsinki University of Technology hip joint simulator Mark III
Slide track	track made on the counterface by a point on the surface of femoral head or acetabular cup due to cyclic relative motion
Force track	track made on the counterface by the point of theoretical joint contact resultant force
Aspect ratio	major dimension divided by minor dimension of a slide track figure
a	amount of offset of the rotation-control lever in the BRM simulator
b	horizontal distance of the vertical post, along which the rotation-control lever slides, from the centre of joint in the BRM simulator

(1998) did not use Euler angles but a fixed Cartesian coordinate system and apparently, they did not verify their results experimentally.

The same verified method of computation (Saikko and Calonius, 2002) was now applied to eight contemporary hip simulator designs, which were not included in the earlier paper. Every track was checked with two alternative methods of computation. The selection of simulators, which has now been analysed, comprises almost all hip simulator test stations currently in use around the world.

2. Methods

The method of computation and its verification was described in detail in an earlier paper (Saikko and Calonius, 2002). The eight simulator designs analysed in the present study are summarised in Table 1, and their motion waveforms are shown in Fig. 1. There are at least four different versions of the BRM simulator, three commercial (‘MMED’, ‘MTS’ and ‘SW’), and one academic (Saikko and Ahlroos, 1999). The case computed in the present study corresponds to the

Table 1
Summary of contemporary hip simulators

Design	Euler sequence and partition of rotations, and classification of axes	Direction of load, and component relative to which it is fixed		Assumed position or neutral position in computation		Reference
				Head axis	Cup	
BRM offset lever	$FE_{h,s} \rightarrow AA_{h,m} \rightarrow IER_{h,m}$	V	c	V	H	Present study, see Fig. 5
AMTI	$AA_{c,m} \rightarrow FE_{c,s} \rightarrow IER_{h,s}$	V	h	V	H	Bragdon et al. (1996)
Munich	$FE_{c,m} \rightarrow AA_{c,m} \rightarrow IER_{c,s}$	V	h	45°	45°	Ungethüm (1976)
Leeds Mk I	$IER_{c,s} \rightarrow FE_{h,s} \rightarrow AA_{h,m}$	Changing	Neither	45°	45°	Dowson and Jobbins (1988)
ISO/DIS 14242-1	Not specified	V	c	30°	30°	Draft ISO/DIS 14242-1 (2001)
Durham Mk II	$IER_{c,s} \rightarrow FE_{h,s}$	V[a]	h	45°	45°	Smith and Unsworth (2001)
Leeds Mk II	$IER_{c,s} \rightarrow FE_{h,s}$	V	c	45°	45°	Barbour et al. (1999)
ProSim	$IER_{c,s} \rightarrow FE_{h,s}$	V[a]	h	V	35°	Goldsmith and Dowson (1999)
HUT-3[b]	$IER_{c,s} \rightarrow AA_{h,s} \rightarrow FE_{h,m}$	12° to V	c	45°	45°	Saikko (1996)
BRM zero-offset lever[b]	$FE_{h,s} \rightarrow AA_{h,m}$	V	c	V	H	Saikko and Ahlroos (1999)

Note: h, head; c, cup; s, stationary axis; m, moving axis; V, vertical; H, horizontal.
[a] In neutral position of FE cradle.
[b] Included here for comparison; their slide tracks were computed earlier, Saikko and Calonius (2002).

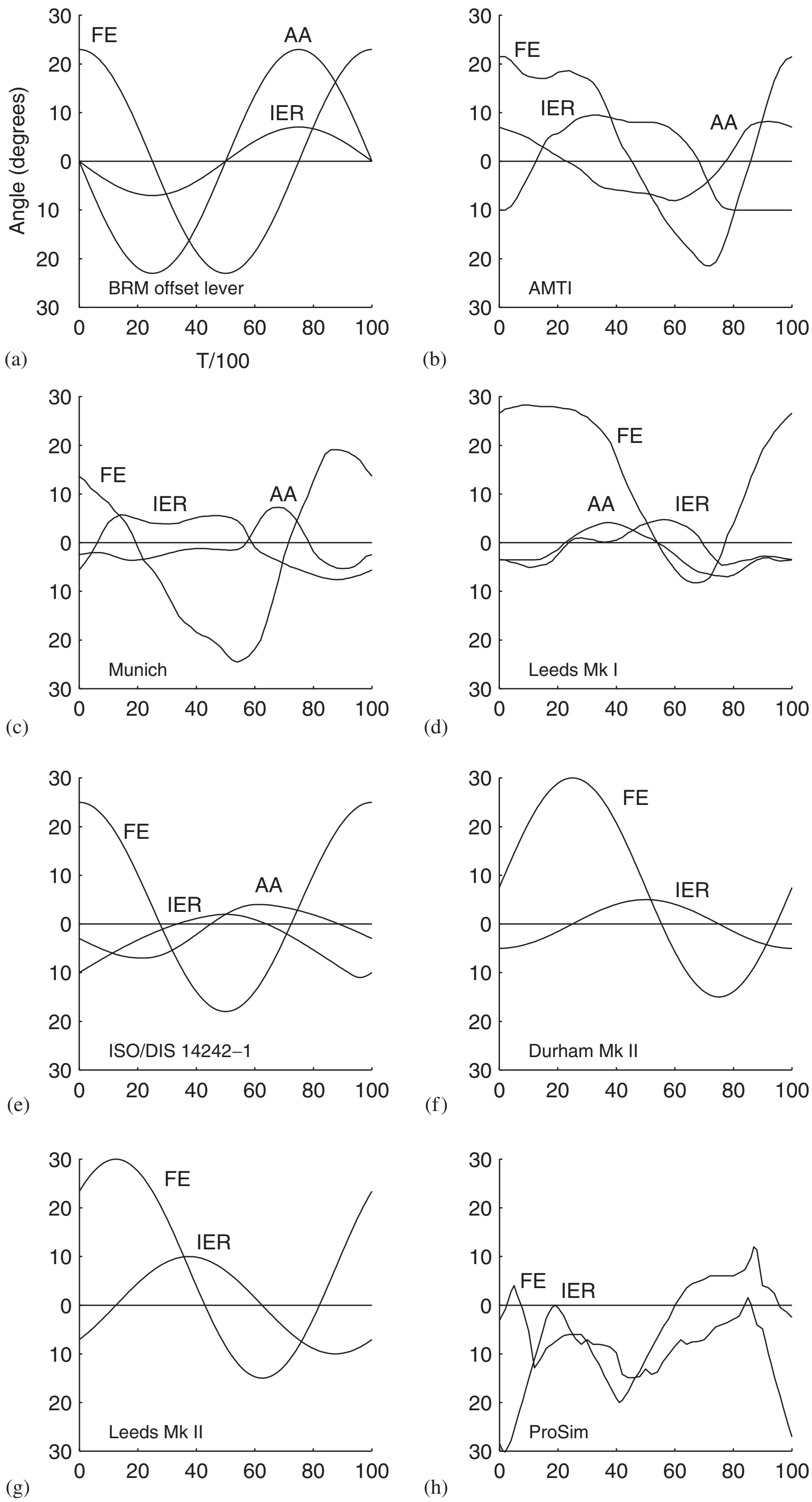

Fig. 1. Motion waveforms used in computation of slide tracks: (a) BRM with offset lever; (b) AMTI; (c) Munich; (d) Leeds Mk I; (e) ISO/DIS 14242-1; (f) Durham Mk II; (g) Leeds Mk II; and (h) ProSim. Positive angle represents flexion, abduction and internal rotation, and negative angle represents extension, adduction and external rotation.

commercial versions, all of which have a lever with offset, that is, the axis of the lever does not go through the centre of the joint. Such a lever does not completely prevent the rotation about the leaning axis, and therefore a third motion component, internal–external rotation (IER), is generated, having the same phase as abduction–adduction (AA) (Fig. 1a). The amplitude of IER depends on the value of offset a and on the horizontal distance of the vertical post from the centre of joint b (Fig. 2), the amplitude being $2\arcsin(a\tan 23^\circ/b)$. When $a = 20$ and $b = 65$ mm, the amplitude is 15°, the value used in the present computation. The amplitude was checked experimentally using an angle rule. Although the arrangement of the components, upright vs. inverted, vary in the commercial versions, the only effect this has on the slide tracks is that the head and cup patterns swap over, because two spheres are assumed to slide against each other in any case. The head track pattern in a version with moving head is identical to the cup track pattern in a version with moving cup, and vice versa.

The motion waveforms were prepared by scanning the published waveforms, and discretising them using 100 points per cycle, at intervals of $T/100$. The BRM waveforms, however, were based on Dr. Saikko's own analysis of the device. In the cases of ISO/DIS 14242-1, Durham Mk II and Leeds Mk II, trigonometric functions, which met the requirements regarding angle values at specified points of time, were generated and used. The problem with most published waveforms was that they represented the set value cycles of the servo-control system, not the true, measured motions, as in Saikko (1996). The delay of the servo-control affects neither the track size nor its shape, but the attenuation does decrease the track size. In the case of Leeds Mk I simulator, the problem was solved so that the set value waveforms presented in Fig. 2 of Dowson and Jobbins (1988) were transformed into true value waveforms using Fig. 7 of the same article, which shows, without scales, the set value and true angular position signals

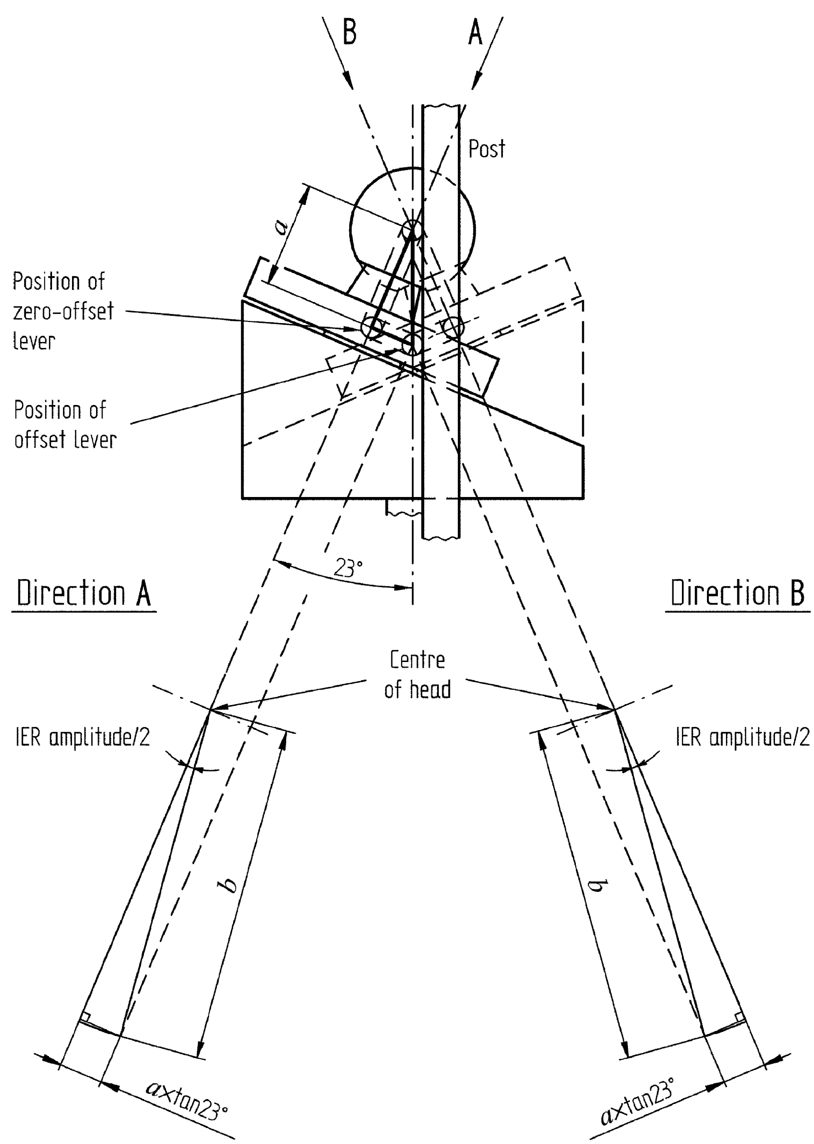

Fig. 2. Illustration showing difference between zero-offset and offset levers in BRM simulator. When lever has offset a, there is sinusoidal IER with amplitude of $2\arcsin(a\tan 23^\circ/b)$, where b is horizontal distance of vertical post from centre of head. If lever has no offset, there is no IER.

together. With the Durham Mk II simulator, two IER amplitudes have been used, 10° and 20°. The former, being more physiological, was selected for the present computation. In most papers, the signs of the AA and IER are ambiguous. The direction mentioned first, e.g. adduction in the Nomenclature 'Add./Abd.' used by Ramamurti et al. (1998), was assumed to correspond with the positive y-axis in the paper in question. If there was no indication of directions, as in the Nomenclature 'rotation' used by Dowson and Jobbins (1988), it was assumed, based on a gait study (Johnston and Smidt, 1969), that internal rotation reaches an extreme value during the support phase.

Not only very different waveforms (Fig. 1), but also different Euler sequences of rotations have been used in existing simulators (Table 1), according to the personal preferences of the designers. The general principle for the determination of the Euler sequence of rotations for any simulator design was presented in Saikko and Calonius (2002). The determination of the Euler sequence of the AMTI simulator is given here as an example. The innermost cradle to which the cup is fixed in the AMTI simulator, makes the AA. This cradle moves together with the flexion-extension (FE) shaft, the axis of which is horizontal and stationary. The IER is made by the head about a vertical, stationary axis. Therefore, since the AA changes the position of both the FE and IER axes relative to the cup, and the FE changes the position of only the IER axis relative to the cup, but the IER does not change the position of any axis relative to the cup, the sequence is AA→FE→IER. Note that the FE, AA and IER of the simulator correspond to the orthopaedic FE, AA and IER only if the sequence is FE→AA→IER. Therefore, the three-dimensional joint motion found from a biomechanical study cannot be reproduced with the simulator by simply reproducing each of the three waveforms by the three rotations of the simulator, if the sequence of the simulator differs from that used in the biomechanical study in question.

In some of the articles describing the simulators, the positions of the head axis and of the cup were not specified. In those cases, the assumed positions used in the computations (Table 1) may differ from those actually used in these simulators. However, this has no effect on the shape and size of individual slide tracks, nor on the track pattern as a whole. It only affects the position of the computed pattern relative to the equator circle shown in Fig. 3. The same holds true for possible anteversion orientation of the cup.

The Leeds Mk I simulator is unique in the sense that with its three-axis loading system, not only the magnitude, but also the direction of the resultant load L can be continuously varied. However, the simulator has been mainly used with the vertical loading cylinder alone, the other two being disconnected. Hence, the location of the force track in the present computation was based on the assumption that the direction of load was vertical, and fixed relative to the cup, as in Mk II.

Finally, an additional verification for the BRM simulator with two different levers was done with a stationary drawing pen, which drew tracks on moving heads.

3. Results

The flattened slide track patterns computed for femoral heads and acetabular cups are shown in Fig. 3. Note that if the direction of load L is fixed relative to the cup, the force track is on the head, and if the direction of load is fixed relative to the head, the force track is on the cup. Considerable differences were found in the slide tracks between the simulators. The force tracks together with their lengths are collected in Fig. 4. The force track shapes were circle (BRM), leaf (Munich), irregular oval (AMTI, Leeds Mk I), ellipse (ISO/DIS 14242-1, HUT-3), figure of eight (Durham Mk II), straight line (Leeds Mk II), and 'twig' (ProSim). By far the longest force track, $2.46r$, was that of the BRM simulator, having also the lowest aspect ratio (1.0). A tangent of the track indicates the instantaneous direction of sliding. Therefore, a circle (Fig. 4a) means that the friction vector τ_μ rotates about the load axis at nearly constant angular velocity, an ellipse (Fig. 4e and i) that the rotation of τ_μ substantially accelerates and decelerates twice per cycle, rotation still occurring in one direction only, a figure of eight (Fig. 4f) that the accelerating and decelerating rotation of τ_μ changes its direction twice per cycle, an irregular shape (Fig. 4b–d, h and j) that quick changes occur in the angular velocity of the rotation of τ_μ, and a straight line (Fig. 4g) that τ_μ has two opposite directions only, the change between them at reversal being instantaneous. Generally, a head track was similar to the corresponding cup track, but their positions were opposite. However, in the special cases of simple sinusoidal motion waveforms (BRM, Durham Mk II, Leeds Mk II), a figure of eight corresponded to a line, and vice versa. If the cup was inclined relative to the horizontal plane, the 'inferior' zone (Fig. 3) is the least important with respect to wear, because the cup is not likely to be in contact with the head there. The difference in the BRM simulator between the two lever cases was verified by a stationary drawing pen, which showed the inclination and shift of the track figures, but constancy of the force track (Fig. 5).

4. Discussion

Femoral head and acetabular cup slide tracks have now been computed for 10 different hip simulator

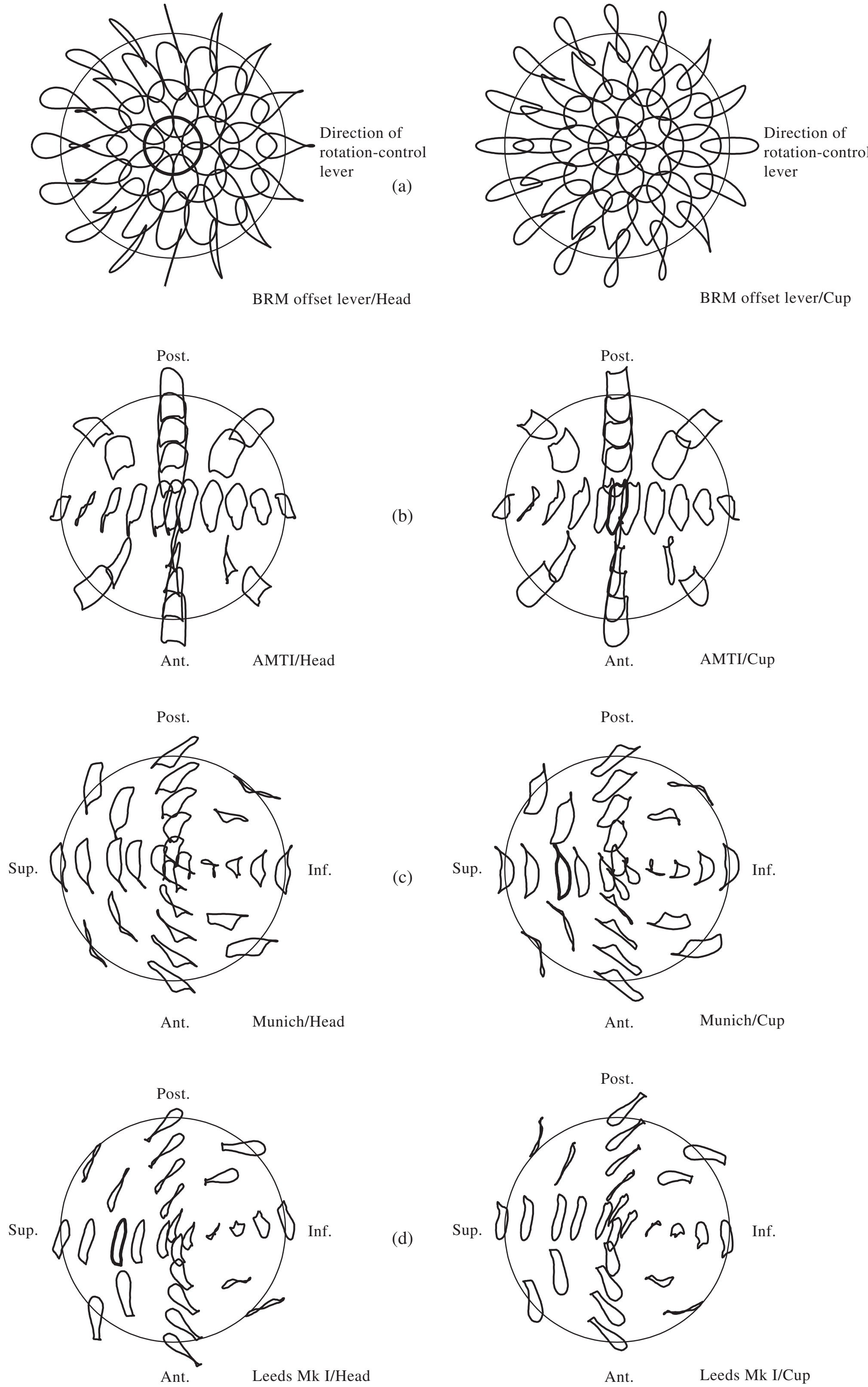

Fig. 3. Computed slide tracks of selected points on flattened hemisphere surface of femoral head (left), and acetabular cup (right), (a) BRM with offset lever, (b) AMTI, (c) Munich, (d) Leeds Mk I, (e) ISO/DIS 14242-1, (f) Durham Mk II, (g) Leeds Mk II, and (h) ProSim. Force track drawn with thicker line. Hemispheres have been flattened so that shapes and sizes of slide tracks are not distorted. Radial distances correspond to distances measured from pole along spherical surface. Large circle represents equator, but due to flattening, its diameter is πr, not $2r$. In cup patterns, tracks outside equator are only imaginary because there is no cup surface outside equator.

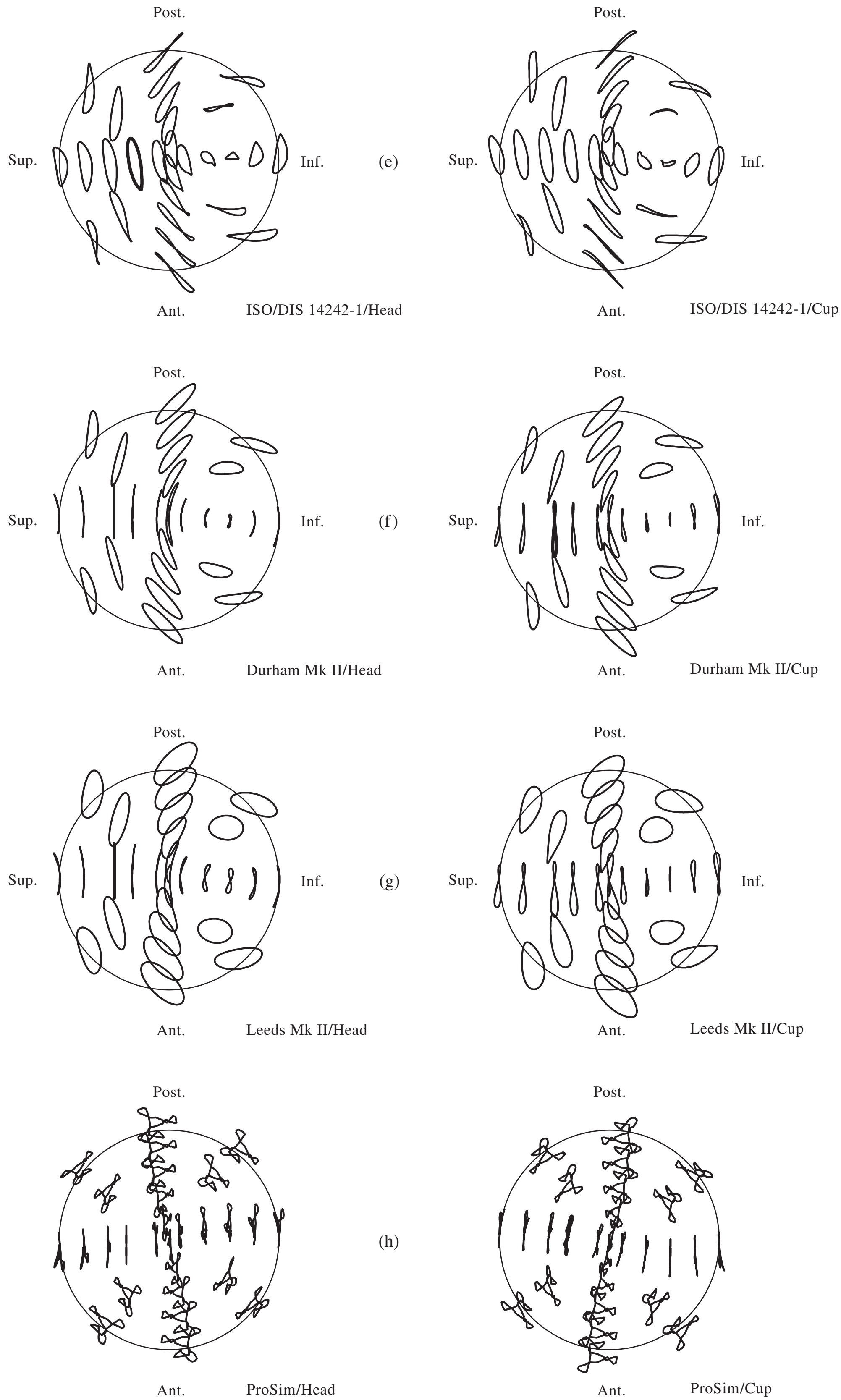

Fig. 3 (*continued*).

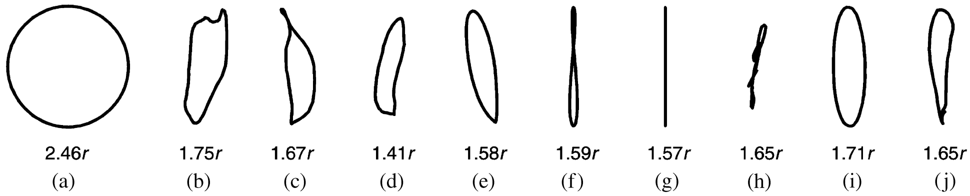

Fig. 4. Force tracks together with their lengths: (a) BRM, (b) AMTI, (c) Munich, (d) Leeds Mk I, (e) ISO/DIS 14242-1, (f) Durham Mk II, (g) Leeds Mk II, (h) ProSim, (i) HUT-3, and (j) gait (Johnston and Smidt, 1969). Flattening as in Fig. 3.

Fig. 5. Additional verification of head tracks in BRM simulator using 28 mm dia. zirconia heads and stationary drawing pen. Station in front has zero-offset lever; straight line is parallel to neck axis, and symmetric figure of eight is on equator. Station in background has offset lever; straight line is inclined relative to neck axis, and symmetric figure of eight is elevated relative to equator. Note also latitudinal (67°) force tracks.

designs, the earlier study (Saikko and Calonius, 2002) included. The selection comprises almost all of the several hundred hip simulator test stations currently in use around the world. This kinematics analysis forms a valuable basis for future studies on the relationship between the type of multidirectional motion and wear. At present, it is known in a general sense only that multidirectional motion is important in order to produce a realistic wear simulation. The type of multidirectional motion, however, varies considerably between simulators and between patients (Bennett et al., 2000), and so does the observed wear. It has been shown that increasing the force track aspect ratio in hip simulators from 1.0 to 3.8 halves the polyethylene wear rate against polished CoCr in serum lubrication (Saikko and Ahlroos, 1999). There are naturally many other variables that affect the wear and complicate the comparison between existing designs. For instance, the variation in degradation behaviour between different serum-based lubricants that have been used in the simulators, is one adverse factor.

The present study is the first to prove that the BRM simulator, which is the most commonly used wear test device for prosthetic hips in the world, and known as biaxial, is actually not biaxial, but three-axial. The breakdown of the obscure motion into FE, AA and IER made it possible to compute the slide tracks correctly (Figs. 1a, 2, 3a, 5 and 6). When the axis of the rotation-prevention lever does not go through the centre of the joint, there is cyclic rotation about the leaning axis, which is true IER by the definition of orthopaedic angles using the Euler sequence FE → AA → IER (Table 1). The simulator should be renamed accordingly, for instance, BRM + IER. In the commercial versions of this simulator, MMED, MTS and SW, the axis of the rotation-prevention lever does not go through the centre of the

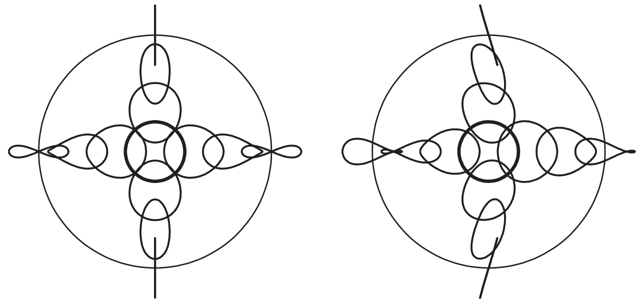

Fig. 6. Illustration of difference in slide tracks between zero-offset (left) and offset lever (right) cases of BRM, using same cup marker points in both cases. Flattened hemisphere surfaces of femoral head. In offset lever case, symmetric figures of eight are not shown, because they are not drawn by points on cup equator as in zero-offset case, but by points located $\arctan(a/b) = \arctan(20/65) = 17^\circ$ from equator, see Fig. 5. Inclination of straight line is also $\arctan(a/b)$.

joint. It is only in the HUT version (Saikko and Ahlroos, 1999) that it does, and it is therefore the only truly biaxial version, the axis of the upper part of the lever always being in one vertical plane. Hence, IER cannot occur. In other cases, the lever should actually not be called a rotation-prevention lever, because it does not completely prevent the IER. A better term would be rotation-control lever. The present slide track pattern (Fig. 3a) clearly differs from that of the zero-offset case (Saikko and Calonius, 2002). The difference is further illustrated in Figs. 5 and 6.

The amplitude of the IER in the BRM simulator depends on the dimensions a and b (Fig. 2). The amplitude, $2\arcsin(a\tan 23^\circ/b)$, increases with increasing a and decreasing b. The diameters of the lever and of the post are unimportant. The IER also affects the sliding speed. Although the difference in the slide track pattern between the offset and zero-offset lever (Saikko and Calonius, 2002) cases is visually distinct (Fig. 6), only a comparative wear test would tell if there is a significant difference also in the primary outcome, the wear behaviour of the prosthesis in question.

In the AMTI simulator (Bragdon et al., 1996), the large size and small aspect ratio of the majority of the tracks are due to the fact that the amplitudes of AA (17°) and IER (20°) are exaggerated compared with gait waveforms (9° and 13°, respectively, middle cycle in Fig. 3 of Johnston and Smidt, 1969). The present tracks differ from those computed by Ramamurti et al. (1998). As was explained in the earlier study (Saikko and Calonius, 2002), the differences are likely to be due to the different coordinate systems used. Ramamurti et al. (1998) did not use Euler angles, but a fixed Cartesian coordinate system. Orthopaedic angles are, however, based on Euler angles, not on a Cartesian coordinate system, and the correct sequence of rotations is crucial. All three axes cannot be perpendicular to each other all the time during the running of the simulator. Moreover, the present method of computation was verified. In the papers by Ramamurti et al. (1996, 1998), there is no mention of any verification. In the two-axis simulators Durham Mk II, Leeds Mk II and ProSim, the two axes are perpendicular to each other all the time, the IER axis of the cup being always vertical, and the FE axis of the head being always horizontal. If there is a third axis in a simulator with two stationary axes, the third axis must move together with either the cup (AMTI) or the head (Leeds Mk I, HUT-3).

The Munich three-axis simulator (Ungethüm, 1976) is the only gimbal-type simulator in which the Euler sequence of rotations is, according to the definition of orthopaedic angles, $\mathrm{FE} \rightarrow \mathrm{AA} \rightarrow \mathrm{IER}$. Interestingly, all three rotations are made by the cup, the femoral component being stationary, and the only stationary axis being the IER. Nevertheless, it is the relative motion that is important tribologically, not the absolute motion of each component. The structure of the Munich simulator deviates from the ISO/DIS 14242-1 specifications mainly in the sense that the direction of load is fixed relative to the head. The standard specifies the direction of load to be fixed relative to the cup. At present, however, it is not known whether this aspect has a significant effect on the wear behaviour of any type of total hip prosthesis. The stem in the leaf-shaped tracks produced by the Munich simulator is caused by the quick and large rise and fall of the AA angle during the swing phase. Such high accelerations are also a source of troublesome vibrations in simulators. The Munich simulator is especially known for the extensive studies of alumina-on-alumina prostheses (Walter, 1997).

There is a striking similarity between the slide tracks produced by the ISO/DIS 14242-1 specification and the HUT-3 simulator (Saikko and Calonius, 2002). At present, however, there is no scientific article describing a simulator that would meet all the requirements of the ISO/DIS 14242-1 standard. Oddly enough, the standard does not specify the Euler sequence of rotations, although it is highly detailed in many other respects. In the present computations, the most logical sequence, FE→AA→IER, was assumed. If a device having a different sequence is built, the slide tracks will differ from the present ones. There are six possible sequences. Hence, six simulators with different sequences can be built, and all of them can be claimed to function 'according to the ISO/DIS 14242-1'. In the strict sense, the sequence should be FE→AA→IER, because only then do the FE, AA, and IER of the simulator correspond to the established system of orthopaedic angles. For example, if the sequence is AA→FE→IER, the FE of the simulator is not the same FE as that used in the definition of hip joint motion in orthopaedic biomechanics, no matter how meticulously the waveform itself is reproduced in the simulator.

The Durham Mk II simulator (Smith and Unsworth, 2001) and the Leeds Mk II simulator (Barbour et al., 1999) had tracks of very high aspect ratio on the zone of the high contact pressure. The tracks became elliptical towards the lower contact pressure zone. With polyethylene, a linear track is known to result in wear rates two orders of magnitude lower than those produced by aspect ratios of the order of 1–4 (Saikko and Ahlroos, 1999). It is therefore possible that in these two simulators, the wear on the high contact pressure zone is reduced. The two Mk II simulators resemble each other, the biggest difference being that in the Durham simulator, the direction of load is fixed relative to the head, whereas in the Leeds simulator, it is fixed relative to the cup. However, when a head track, for instance the force track in Fig. 3g, in a two-axis simulator of the type specified in Table 1 is linear, the sliding relative to the cup, at the marker point in question, i.e., the point of resultant force, is not exactly reciprocating. This is because the IER of the cup occurs about the point of resultant force. The IER does not affect the shape of the force track. In such a case, the rotation of τ_μ relative to the cup at this point is described (although it may at first appear paradoxical) by the corresponding cup track, which is a narrow figure of eight due to the $\pi/2$ phase difference between the FE and IER. Relative to the head, the sliding is truly reciprocating, τ_μ having two opposite directions only. The same phenomena can be seen on the equator of the BRM simulator (Fig. 3a). The corresponding cup track of the inclined straight line on the head is the inclined, symmetric figure of eight. Naturally, the equator of the cup in the BRM simulator, when the cup is located horizontally above the head, is not very important tribologically because the contact pressure axisymmetrically approaches zero towards the equator.

The Durham Mk II, Leeds Mk II and BRM simulators are in fact special cases due to their simple sinusoidal motion waveforms. In the BRM simulator for instance, the centre tracks, the 67° latitude circles, of the head and cup patterns are identical. The IER does not affect them because (I) the pole of the head, which draws the circle on the cup, is on the IER axis, and (II) the pole of the cup, which draws the circle on the head, draws along the 67° latitude only. In a general case, the head track is similar (but not identical) to the corresponding cup track, the opposite position taken into account (Fig. 7). The similarity is maximal when the difference in locations is minimal. In the present study however, the head and cup marker points were selected so that the points met in the neutral position of the simulator, not so that the difference in the locations of the head and cup tracks would be minimal. The neutral position was chosen on the basis of clarity: in the neutral position, the FE, AA and IER angles were zero. The simulators were actually never in such a position during the cycle. This explains why the location of the head track in some cases clearly differed from that of the corresponding cup track, see, e.g., the narrow equator tracks of the Leeds Mk I simulator in Fig. 3d. The difference in the location between these head and cup tracks was due to the highly asymmetric location of the FE waveform relative to the neutral position (Fig. 1d).

The slide tracks that differed the most from the others were those produced by the ProSim device (Goldsmith and Dowson, 1999). Its motion waveforms were mentioned to be from Paul (1967), but the subject of that study is load, not motion. Hence, it is unclear where such peculiar, jerky motion waveforms originate. The

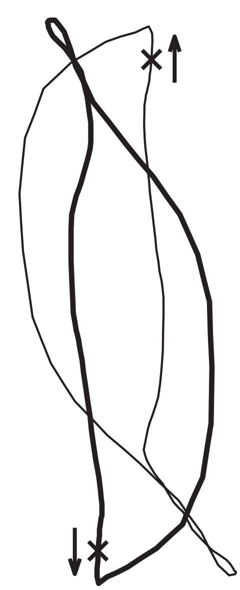

Fig. 7. Force track (thicker line) of Munich simulator and corresponding head track superimposed. Tracks are similar but not identical. Cup marker point selected only for this illustration so that difference in track locations is minimal. Shown are also marker points at arbitrary moment, and direction of sliding. Reason for difference in shape can be understood by considering stems of leaf-shaped tracks: stems are drawn at same time, but on different locations. Making stems meet by selecting cup marker point differently would increase similarity of stems, but similarity towards apex parts of leaves would again decrease.

ProSim device had the highest cumulative rotation angle of τ_μ per cycle, manifested as several loops in the tracks, which probably accelerates wear. On the other hand, the tracks on the high contact pressure zone had high aspect ratios, which may be counteractive regarding the total wear, as in the Mk II devices. The sharp reversals of motion certainly cause severe vibration problems, which may even affect wear.

One noteworthy aspect in the computation of sequential rotations using Euler angles is that the same result is obtained using an *inverted* sequence and a fixed Cartesian coordinate system (Craig, 1989). All the cases of the present study and of the earlier one (Saikko and Calonius, 2002) were additionally computed using inverted sequences and the Cartesian coordinate system. All tracks proved to be identical to those computed using the true sequences and Euler angles. For instance, Euler angles and the sequence IER→AA→FE gives the same correct result for the HUT-3 simulator (verified by carved grooves) as the Cartesian coordinate system and the sequence FE→AA→IER. The sequence is nevertheless crucial with both coordinate systems. This was checked by varying the sequence. With both systems, changing the sequence resulted in distinct changes in tracks, which contradicts the claim by Ramamurti et al. (1996) that all six sequences result in 'virtually identical' tracks. Note that the present tracks were computed with three different methods, and the result was always the same. This together with the experimental verification done makes the results highly reliable.

It would be most interesting to compare the wear produced by the contemporary simulators with a view to finding relationships between the slide track pattern and wear. This would require that similar specimens, lubrication, temperature and load were used. Such a comparison is, however, not yet possible because the tests reported in the publications greatly differ from each other regarding the materials, the type, amount and dilution of serum, heating, frequency, etc. The relative importance of each variable is not known precisely. Hence, the significance of slide tracks in the difference in wear between designs cannot, unfortunately, be quantified at present. Moreover, there are no published wear data produced in the test conditions described in the ISO/DIS 14242-1 standard. However, the ISO/DIS 14242-1 slide tracks were strikingly similar to those produced by the validated (Saikko and Ahlroos, 1999; Calonius and Saikko, 2002) HUT-3 simulator (Saikko and Calonius, 2002). It is therefore likely that the ISO/DIS 14242-1 test conditions will produce realistic wear. Nevertheless, now that the slide tracks of the majority of existing hip simulators have been computed, a multi-laboratory test programme using similar specimens, lubrication, temperature and load, would produce extremely valuable information, not only for the progress of joint simulator design, but also for the better understanding of wear phenomena in prosthetic joints.

Acknowledgements

The study was funded by the Academy of Finland (grant no. 43328 and Dr. Saikko's Academy Research Fellowship).

References

Barbour, P.S., Stone, M.H., Fisher, J., 1999. A hip joint simulator study using simplified loading and motion cycles generating physiological wear paths and rates. Journal of Engineering in Medicine 213, 455–467.

Bennett, D.B., Orr, J.F., Baker, R., 2000. Movement loci of selected points on the femoral head for individual total hip arthroplasty patients using three-dimensional computer simulation. Journal of Arthroplasty 15, 909–915.

Bragdon, C.R., O'Connor, D.O., Lowenstein, J.D., Jasty, M., Syniuta, W.D., 1996. The importance of multidirectional motion on the wear of polyethylene. Journal of Engineering in Medicine 210, 157–165.

Calonius, O., Saikko, V., 2002. Analysis of polyethylene particles produced in different wear conditions in vitro. Clinical Orthopaedics and Related Research 399, 219–230.

Craig, J.J., 1989. Introduction to Robotics: Mechanics and Control, 2nd Edition. Addison-Wesley Publishing Company Inc., Reading, MA, p. 49.

Dowson, D., Jobbins, B., 1988. Design and development of a versatile hip joint simulator and a preliminary assessment of wear and creep in Charnley total replacement hip joints. Engineering in Medicine 17, 111–117.

Goldsmith, A.A.J., Dowson, D., 1999. A multi-station hip joint simulator study of the performance of 22 mm diameter zirconia-ultra-high molecular polyethylene total replacement hip joints. Journal of Engineering in Medicine 213, 77–90.

ISO/DIS 14242-1 Draft International Standard, 2001. Implants for surgery—wear of total hip joint prostheses—Part 1: loading and displacement parameters for wear-testing machines and corresponding environmental conditions for test.

Johnston, R.C., Smidt, G.L., 1969. Measurement of hip-joint motion during walking—evaluation of an electrogoniometric method. Journal of Bone and Joint Surgery 51-A, 1083–1094.

Paul, J.P., 1967. Forces transmitted by joints in the human body. Proceedings of the Institution of Mechanical Engineers 181 (Part 3J), 8–15.

Ramamurti, B.S., Bragdon, C.R., O'Connor, D.O., Lowenstein, J.D., Jasty, M., Estok, D.M., Harris, W.H., 1996. Loci of movement of selected points on the femoral head during normal gait. Journal of Arthroplasty 11, 845–852.

Ramamurti, B.S., Estok, D.M., Jasty, M., Harris, W.H., 1998. Analysis of the kinematics of different hip simulators used to study wear of candidate materials for the articulation of total hip arthroplasties. Journal of Orthopaedic Research 16, 365–369.

Saikko, V., 1996. A three-axis hip joint simulator for wear and friction studies on total hip prostheses. Journal of Engineering in Medicine 210, 175–185.

Saikko, V., Ahlroos, T., 1999. Type of motion and lubricant in wear simulation of polyethylene acetabular cup. Journal of Engineering in Medicine 213, 301–310.

Saikko, V., Calonius, O., 2002. Slide track analysis of the relative motion between femoral head and acetabular cup in walking and in hip simulators. Journal of Biomechanics 35, 455–464.

Smith, S.L., Unsworth, A., 2001. A five-station hip joint simulator. Journal of Engineering in Medicine 215, 61–64.

Ungethüm, M., 1976. Tribologisch-biomechanische Untersuchungen für den totalen Gelenkersatz der menschlichen Hüfte. Doctoral Dissertation, Rheinisch-Westfälische Technische Hochschule Aachen.

Walter, A., 1997. Investigations on the wear couple Biolox forte/Biolox forte and earlier alumina materials. In: Puhl, W. (Ed.), Performance of the Wear Couple Biolox Forte in Hip Arthroplasty. Ferdinand Enke Verlag, Stuttgart, pp. 123–135.